

Effect of Palm Fiber on Photo and Thermo-Degradation of Polyethylene Composites

Wirasak Smithipong¹, Rungsima Chollakup^{1,2,*},
Wuttinan Kongtad¹ and Florence Delor-Jestin^{2,3}

ABSTRACT

Polyethylene/palm fiber composites (PEP) were prepared by blending low density polyethylene (PE) and palm fibers (diameter < 1 mm) in a twin-screw extruder. Thin films of PEP at 0–30% fiber weight were either exposed to accelerated artificial photo-ageing ($\lambda > 300$ nm, 60 °C) or to thermo-oxidation at 100 °C in an aerated oven. Infrared (IR) spectra after photo-oxidation showed that the incorporation of fibers in PE increased its degradation rate with the formation of carbonyl and vinyl groups. A decrease was observed in the aromatic C=C absorption IR peaks of the lignin structure in the PEP composites. This indicated that the lignin structure in the fibers was photo-oxidized and produced radical species for oxidation. Crystallinity change of the PEP composites, analyzed using differential scanning calorimetry, tended to increase upon photo- and thermo-ageing. This effect could be explained by chain scissions involved in the oxidation process, as the shorter chains of PE would have a higher mobility, allowing the reorganization of the PE matrix. Compared to thermo-degradation, the amount of vinyl groups remained constant indicating no reaction of the ketones in a Norrish type II process. The higher thermo-oxidation rate in PEP composites may be a result of radical species of cellulose and hemicellulose degradation in palm fibers.

Keywords: polyethylene (PE), palm fiber, photo-degradation

INTRODUCTION

Cellulose fiber based composites have been applied commercially in the construction and automotive industries (Mohanty *et al.*, 2000). Durability to outdoor environments for these cellulose fiber-based composites was of concern, especially to solar light. Attention has mainly focused on the photo-degradation of wood-polyethylene (PE) submitted to natural and

artificial weathering (Stark and Matuana, 2004; Stark, 2006; Ndiaye *et al.*, 2008; Taib *et al.*, 2010). These studies on wood flour or cellulose-fiber-reinforced PE have focused either on changes in the surface chemistry with IR spectroscopy or on mechanical properties. Most studies found that the fiber inclusion accelerated the oxidation rate upon ultraviolet (UV) to visible light exposure (Stark and Matuana, 2004; Stark, 2006; Ndiaye *et al.*, 2008). Stark and Matuana (2004) found

¹ Kasetsart Agricultural and Agro-Industrial Product Improvement Institute (KAPI), Kasetsart University, Bangkok 10900, Thailand.

² Clermont Université, Université Blaise Pascal, Institut de Chimie de Clermont-Ferrand (ICCF), CNRS UMR 6296, BP 10448, F-63000, France.

³ Clermont Université, ENSCCF, BP10448, F-63000, Clermont-Ferrand, France.

* Corresponding author, e-mail: aaprmc@ku.ac.th

that the carbonyl index of the wood flour/high density polyethylene (HDPE) was higher than that of the HDPE. This was explained by the fact that lignin in wood flour is very sensitive to UV light degradation (George *et al.*, 2005).

In the current study, bleached palm fiber from wastes generated from oil production in Thailand were chosen to reinforce the PE matrix. The objective of this work was to investigate the effect of small fiber particle inclusion (1 mm size) on the chemical structure and crystallinity of these cellulose fiber-reinforced PE composites after exposure to accelerated photo- and thermo-ageing. Photo-ageing conditioning was performed under UV-light irradiation at 60 °C. Thermo-oxidation used an aerated oven at 100 °C. The chemical modifications of the composites were investigated using infrared spectroscopy. Differential scanning calorimetry (DSC) was used to analyze the change in the crystallinity during photo- and thermo-oxidation.

MATERIALS AND METHODS

Materials

Composite preparation

Palm fruit bunches from an oil production factory were used as the source of the palm fibers. Palm fibers were extracted from agricultural wastes according to Chollakup *et al.*, (2013). Briefly, palm fruit bunches were treated with 25% NaOH on a weight basis (a liquor ratio of NaOH to fiber of 15:1) at 100 °C for 3 hr. Then, the alkaline treated coir fibers were bleached at 100 °C for 2 hr using 30% hydrogen peroxide at a liquor ratio of solution to fiber of 30:1.

Fibers were ground into powder and passed through a 20-mesh sieve using a rotor mill (Pulverisette14; Fritsch; Idar-Oberstein, Germany) at a speed of 16,000 revolutions per minute (rpm). Polyethylene (Dow LDPE 320E, PE), with a density of 0.925 g.cm⁻³ and a melt flow index of 1.0 g per 10 min, was supplied by the Dow Chemical Company (Edegem, Belgium). The palm fibers

at 5-20% by fiber volume were blended with PE granules in a twin-screw extruder (Haake Minilab; Thermo Scientific; Karlsruhe, Germany) at 170 °C with a roller speed of 90 rpm for 10 min. Then the extrudates were cut into palettes and pressed at 150 °C for 1 min under a pressure of 20 MPa. Composite films were obtained with a thickness of 90-130 µm.

Composite ageing

Irradiation was carried out in a SEPAP 12/24 unit. This tool had been designed for the study of polymer photo-degradation in artificial ageing conditions corresponding to medium accelerated conditions (Lemaire *et al.*, 1981). For these experiments, the temperature at the surface of the samples was fixed at 60 °C. Low temperature thermo-oxidation experiments were carried out in a ventilated oven at 100 °C.

Analytical method

Infrared and ultraviolet spectroscopy

Infrared spectra were recorded in transmission mode with a Nicolet 760-FTIR spectrophotometer (Thermo Fisher Scientific Co.; Waltham, MA, USA) with OMNIC software (version 8.3; Thermo Fisher Scientific Co.; Waltham, MA, USA). Spectra were obtained using 32 scans and a 4 cm⁻¹ resolution. To avoid differences due to film thickness and PE contents, the normalized absorbance ($\Delta I_{normalized}$) was reported according to Equation 1 (Morlat-Therias *et al.*, 2008):

$$\Delta I_{normalized} = \frac{\Delta I_v}{I_{ref}} \quad (1)$$

where ΔI_v corresponds to the intensity difference of the band at any wave number from an initial time and I_{ref} corresponds to the intensity of the reference band at 720 cm⁻¹, attributed to C-H rocking (Pagès *et al.*, 1996). In addition, UV spectroscopy using a UV-2101PC spectrophotometer (Shimadzu; Kyoto, Japan) was used to study the change in UV absorption after photo and thermo-degradation.

Differential scanning calorimetry

The melting temperature and heat of

fusion of the composites were determined using DSC (DSC822; Mettler; Toledo, OH, USA). Samples were first run from 25 to 200 °C at 10 °C per min to remove any thermal history. Then, the samples were cooled to room temperature at 10 °C per min to record the crystallization behavior before reheating to 100 °C at 20 °C per min to trace the melting behavior. The crystallinity of the composites was calculated according to Equation 2:

$$\chi(\%) = 100 \times \frac{\Delta H_f}{\Delta H_f^0} \quad (2)$$

where ΔH_f^0 and ΔH_f are the heat of fusion of the 100% crystalline polymer and composites, respectively. ΔH_f^0 is 290 J.g⁻¹ for PE.

RESULTS AND DISCUSSION

Figure 1 shows the IR spectra of the PE composites at different fiber contents before ageing. The IR spectra of the PE composites contain additional absorption bands at 3000–3500 cm⁻¹ attributed to hydroxyl linkages (hydrogen bonds of cellulose, alcohols, hydroperoxides, and of water among others), at 1600–1800 cm⁻¹ attributed to conjugated C=O bonding of cellulose and ligno-cellulose, and at 900–1300 cm⁻¹ attributed to C-O vibration (Bajer *et al.*, 2007) compared to the PE spectra. The intensity of these additional bands increased naturally with the fiber

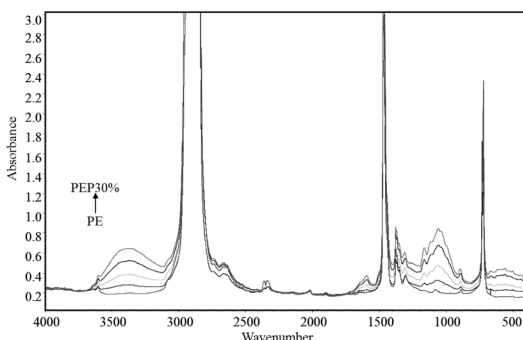


Figure 1 Infrared spectra of polyethylene/palm fiber composites at 0–30% by weight of fiber contents before ageing.

content (before ageing). Figure 2 shows the UV-visible spectra of the PEP films before ageing. This figure shows that cellulose fibers absorb in the UV-visible region at 280 nm and the UV intensity increases with the fiber content. Lignin is the main component of the chemical composition of fiber which absorbs relatively strongly in the UV-visible region (George, 2005). As shown in the results, the lignin content of the palm fiber after bleaching was 10.9%.

As reported for PE (Lacoste and Carlsson, 1992) photo-ageing results in the formation of hydroxyl groups (broad absorption centered at 3430 cm⁻¹), of a carbonyl envelope centered at 1712 cm⁻¹ and a vinyl group (908 cm⁻¹). Figure 3 shows the evolution in the carbonyl domain for the pure PE and PEP composite at 30% by weight. It is noteworthy that the same evolutions were analogous for PEP composites and look like the one observed in a PE film (Lacoste and Carlsson, 1992). For the same time of irradiation, photoproduct quantities are always higher for PEP than for PE (Ndiaye *et al.*, 2008). However the current study found only a decrease in the aromatic C=C absorption band at 1595 and 1506 cm⁻¹ of PEP composites, indicating lignin structures as seen in Figure 3. Decreases in these peaks depended on the fiber content in the composites. For a higher fiber content, a higher rate was obtained (data not shown). The

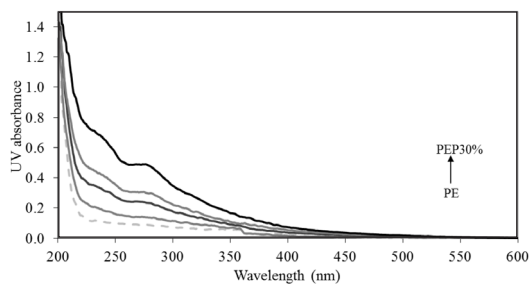


Figure 2 UV (ultraviolet)-visible spectra of polyethylene/palm fiber (PEP) composites at 0–30% by weight of fiber content before ageing (PE = Low density polyethylene).

disappearance of this peak which was seen by the negative absorbance values proved that the lignin structure in fiber was degraded and further oxidized to form paraquinone chromospheres as described by Muasher and Sain (2006). Decreases in the IR spectra of cellulose fibers at 1595 and 1506 cm^{-1} after photo-oxidation was observed on PE/coir fiber composite (Chollakup *et al.*, 2012)

An increase in carbonyl groups formed during photo-ageing in the PE and in PEP composites is shown in Figure 4 which indicates that the oxidation rate of the PEP composites increased with the fiber content. In contrast, the formation of vinyl groups resulting from the decomposition of ketones according to the Norrish II process is the same for PE and PEP composites (data not shown). The formation of vinyl groups indicated that photo-degradation occurred via

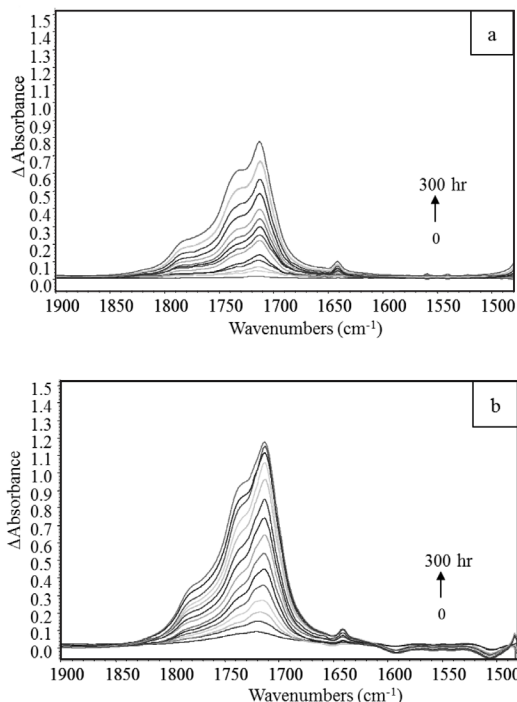


Figure 3 Changes in the infrared spectra of: (a) Low density polyethylene; (b) Polyethylene/palm fiber composites at 30% by weight of fiber content during photo-oxidation in the SEPAP device at $\lambda > 300 \text{ nm}$ and 60°C .

Norrish II reactions, resulting in chain scission (Kaci *et al.*, 2000). Figure 5 shows that the absorbance in the UV domain (less than 300 nm) of the PEP composites increases with ageing time. Increasing UV absorbance resulted from oxidation products upon photo-degradation.

Thermo-degradation occurred over 200 hr due to the tolerance conditions within the polymer bulk at 100°C . Figure 6 shows the changes in the carbonyl spectra of the PE and PEP composite during thermo-oxidation. The oxidation rate after thermo-ageing was higher than that after photo-ageing. There was no change

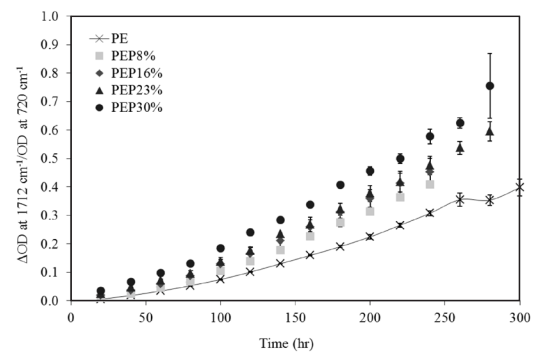


Figure 4 Absorbance changes at 1712 cm^{-1} during photo-oxidation of polyethylene/palm fiber (PEP) composites as a function of ageing time. (OD = the optical density; Vertical error bars indicate $\pm \text{SD}$; PE = Low density polyethylene.)

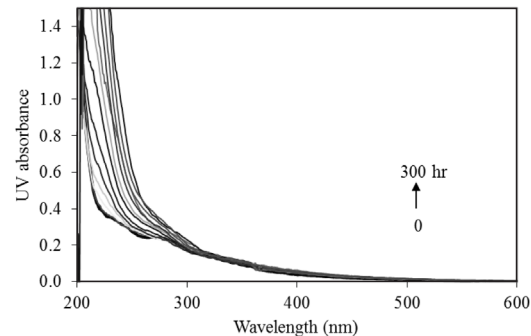


Figure 5 UV (ultraviolet)-visible spectra of polyethylene/palm fiber (PEP) composites at 16% by weight of fiber content during photo-oxidation.

in the vinyl group formation (at 908 cm^{-1}) which was an indication of main scission according to only a Norrish I reaction (data not shown). If the degradation proceeds according to a Norrish II reaction, carbonyl groups and terminal vinyl groups would be produced as was found upon photo-ageing. Increasing the fiber content in the PEP composites produced a distinct increase in carbonyl group formation as shown in Figure 7. However, there was no decrease in the aromatic $\text{C}=\text{C}$ absorption band at 1506 cm^{-1} which indicated that the aromatic lignin in the fiber component is thermally stable. A higher oxidation rate during the thermo-oxidation of the PE composites may have led to the decrease in the degree of polymerization of cellulose or hemicellulose at $100\text{ }^{\circ}\text{C}$ (LeVan, 1989).

Figure 8 shows the change in the UV-

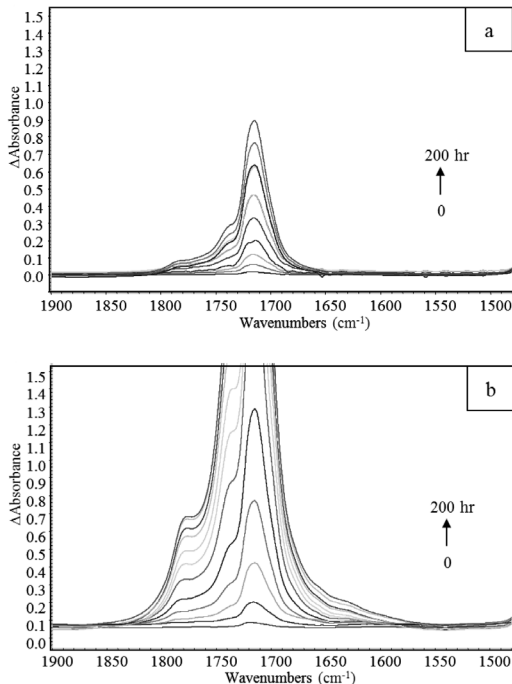


Figure 6 Changes in the infrared spectra at 1712 cm^{-1} of: (a) Low density polyethylene; (b) Polyethylene/palm fiber composites at 30% by weight of fiber content during thermo-oxidation in the oven at $100\text{ }^{\circ}\text{C}$.

visible spectra of the PEP composites at 16% by weight during thermo-oxidation. The absorbance in the UV domain (less than 300 nm) increased with ageing time and especially with absorbance at 280 nm which increased at a higher rate than that of photo-oxidation. This UV result supported the IR results of the PE composites during thermo-ageing.

In photo-ageing, the crystallinity degree of all PE and PEP composite increased as shown in Figure 9a. An increase was observed in the crystallinity degree which tended to a plateau after 200 hr exposure. With progress in the photo-

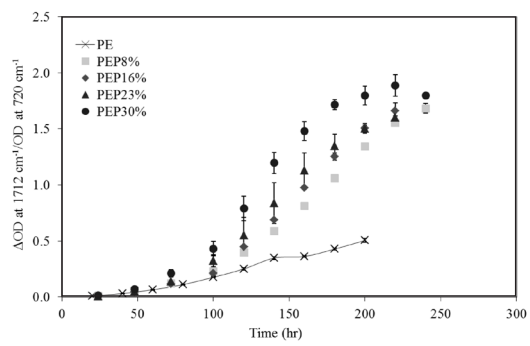


Figure 7 Absorbance changes at 1712 cm^{-1} during thermo-oxidation of polyethylene/palm fiber (PEP) composites and as a function of ageing time. (OD = the optical density; Vertical error bars indicate $\pm \text{SD}$; PE = Low density polyethylene.)

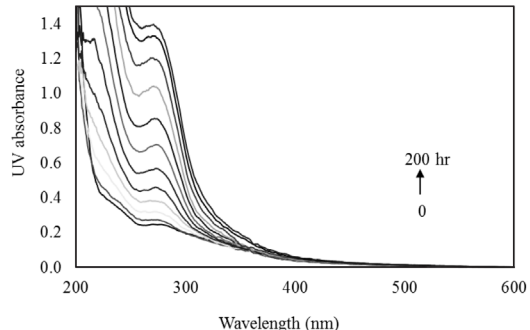


Figure 8 UV (ultraviolet)-visible spectra of polyethylene/palm fiber (PEP) composites at 16% by weight of fiber content during thermo-oxidation.

oxidation process, the number of chain scissions increased with a reduction in the molecular size, which allowed the rearrangement of these shorter molecular chains according to the well known chemi-crystallization process (Wunderlich, 1976). This resulted in an increase in the crystallinity degree for the PEP composites.

With thermo-ageing, no change in crystallinity of PE was found (Figure 9b). The crystallinity degree of the PEP composites produced similar results to photo-ageing. The longer the ageing time, the higher the crystallinity degree obtained for the PEP composites. An increased crystallinity degree was observed only in the initial ageing time (100–200 hr). The longer the ageing time, the more constant the crystallinity degree of the PE composites became. It was hypothesized as described in the photo-ageing above that the molecule segments with bulky and randomly distributed chemical groups can not fit into the crystal lattice. This results in an interruption of the chemi-crystallization (Stark and Matuana, 2004). Furthermore, that rearrangement of the shorter PE molecule should induce the formation of the chemi-crystallinity as explained in the photo-degradation part and result in an increase in the crystallinity of the pure PE. However, the crystallinity change was not found in the pure PE

due to this thermo-ageing condition accelerating further the degradation mechanism in the PE polymer. The chemi-crystallinity of the shorter molecules in the PEP composites was still being formed. In thermal ageing, thermal annealing can also influence the evolution of crystallinity which was not possible during photo-ageing. The effect of the presence of fiber was mainly significant for the evolution of crystallinity during each type of ageing. The influence of small chains in the PEP composites was underlined with spectral analysis and could be one explanation for the crystallinity increase.

Figure 10a presents only Young's modulus of the PE and PEP composite at 5% by weight after photo-oxidation. It can be observed that the Young's modulus of the pure PE increased substantially when ageing time increased. The Young's modulus of the PEP composite tended to increase. The formation of carbonyl and vinyl groups in the PE indicated main-chain scission, as the shorter chains from the photo-oxidation products of the PE have a higher mobility with rearrangement to make the PE molecular chains more crystalline (Stark and Matuana, 2004). Therefore, the Young's modulus of the pure PE increased. However, fiber inclusion in the PE matrix prevented UV absorption of PE,

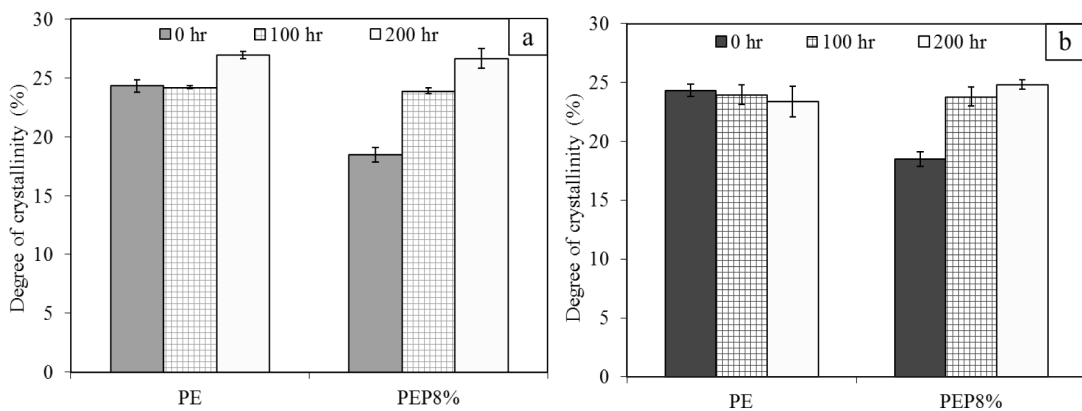


Figure 9 Crystallinity degree of the low density polyethylene (PE) and polyethylene/palm fiber (PEP) composites at 8% by weight after: (a) Photo-ageing; (b) Thermo-ageing. (Vertical error bars indicate \pm SD.)

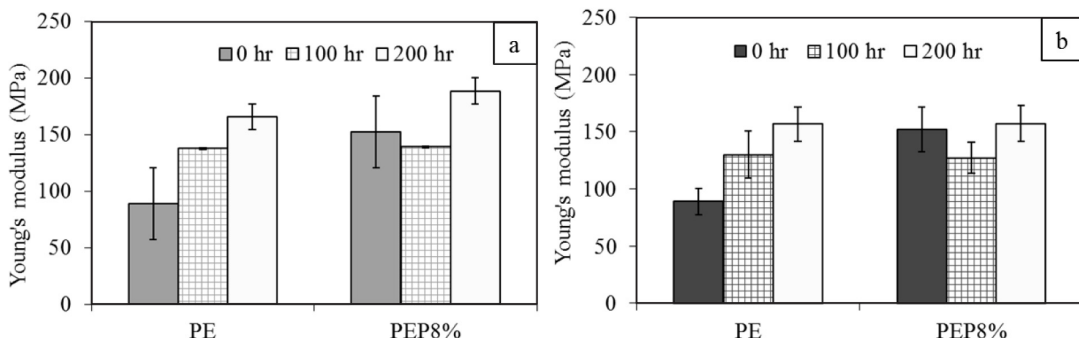


Figure 10 Young's modulus of the low density polyethylene (PE) and polyethylene/palm fiber (PEP) composites at 8% by weight After: (a) Photo-ageing; (b) Thermo-ageing. (Vertical error bars indicate \pm SD.)

consequently, shorter chains of PE were less common in the PEP composite which made it less crystalline compared to the PE. Thus, increasing Young's modulus of the PEP composite after radiation was less influential compared to the PE. After thermo-oxidation, the values of Young's modulus of the pure PE and the PEP composite (Figure 10b) tended to increase with increased ageing time. This would describe the previous results after photo-degradation. However, there was no change in Young's modulus for any of the PEP composites.

CONCLUSION

The palm fiber content incorporated in the PE matrix resulted in changes in the functional groups and crystallinity of the PEP composites after photo- and thermo-ageing. Lignin in the fibers was sensible to UV absorbance which produced radical species and initiated the chain scission of polymers upon photo-oxidation. Upon thermo-oxidation, cellulose and hemicellulose were the main components producing radical species to increase the polymer oxidation. Chemi-crystallization also produced higher crystallization after ageing. This results of this study suggest the addition of UV stabilizer in PEP composites to prevent photo- and thermo-degradation.

ACKNOWLEDGEMENTS

This work was supported by KAPI, Kasetsart University, Bangkok, Thailand and Institut de Chimie de Clermont-Ferrand (ICCF), Le Centre national de la recherche scientifique (CNRS). Universite Blaise Pascal, Clermont-Ferrand, France.

LITERATURE CITED

Bajer, K., H. Kaczmarek, J. Dzwonkowski, A. Stasiek and D. Oldak. 2007. Photochemical and thermal stability of degradable PE/paper waste composites obtained by extrusion. *J. Appl. Polym. Sci.* 103: 2197–2206.

Chollakup, R., W. Smitthipong, W. Kongtud and R. Tantatherdtam. 2013. Polyethylene green composites reinforced by cellulose fibers (coir and palm fibers): effect of fiber surface preparation and fiber content. *J. Adhes. Sci. Technol.* 27: 1290–1300.

Chollakup, R., F. Delor-Jestin, A. Rivaton, S. Therias and J.L. Gardette. 2012. Influence of coir fiber on stability of polyethylene composites exposed to photo and thermo-ageing, p. 131. *In Abstract Book of 7th International Conference on Materials Science and Technology*. June 7-8, 2012. Swissotel Le Concorde, Bangkok, Thailand.

George, B., E. Suttie, E., A. Merlin and X. Deglise. 2005. Photodegradation and photostabilisation of wood - the state of the art. **Polym. Degrad. Stab.** 88: 268–274.

Kaci, M., T. Sadoun. and S. Cimmino. 2000. HALS stabilization of LDPE films used in agricultural applications. **Macromol. Mater. Eng.** 278: 36–42.

Lacoste, J. and D.J. Carlsson. 1992. Gamma-, photo-, and thermally-initiated oxidation of linear low density polyethylene: A quantitative comparison of oxidation products. **J. Polym. Sci. Part A: Polym. Chem.** 30: 493–500.

Lemaire, J., R. Arnaud and J.L. Gardette. 1981. Le vieillissement des polymères: principes d'étude du photovieillissement. **Rev. Gen. Caoutch. Plast.** 613: 87–92. [in French]

Levan, S.L. 1989. **Concise Encyclopedia of Wood & Wood-Based Materials.** 1st ed., Pergamon Press. Elmsford, NY, USA. pp. 271–273.

Mohanty, A.K., M. Misra and G. Hinrichsen. 2000. Biofibers, biodegradable polymers and biocomposites: An overview. **Macromol. Mater. Eng.** 276-277: 1–24.

Morlat-Therias, S., E. Fanton, J.L. Gardette, N.T. Dintcheva, F.P. La Mantia and V. Malatesta. 2008. Photochemical stabilization of linear low-density polyethylene/clay nanocomposites: Towards durable nanocomposites. **Polym. Degrad. Stab.** 93: 1776–1780.

Muasher, M. and M. Sain. 2006. The efficacy of photostabilizers on the color change of wood filled plastic composites. **Polym. Degrad. Stab.** 91(5):1156–1165.

Ndiaye, D., L.M. Matuana, S. Morlat-Therias, L. Vidal, A. Tidjani and J.L. Gardette. 2008. Durability of wood polymer composites: Part 1. Influence of wood on the photochemical properties. **Compos. Sci. Technol.** 68: 2779–2784.

Pageès, P., F. Carrasco, J. Surina and X. Colom. 1996. FTIR and DSC study of HDPE structural changes and mechanical properties variation when exposed to weathering aging during Canadian winter. **J. Appl. Polym. Sci.** 60: 153–159.

Stark, N.M. 2006. Effect of weathering cycle and manufacturing method on performance of wood flour and high-density polyethylene composites. **J. Appl. Polym. Sci.** 100: 3131–3140.

Stark, N.M. and L.M. Matuana. 2004. Surface chemistry and mechanical property changes of wood-flour/high-density-polyethylene composites after accelerated weathering. **J. Appl. Polym. Sci.** 94: 2263–2273.

Taib, R.M., N.S.A. Zauzi, Z.A.M. Ishak and H.D. Rozman. 2010. Effects of photo-stabilizers on the properties of recycled high-density polyethylene (HDPE)/wood flour (WF) composites exposed to natural weathering. **Malaysian Polym. J.** 5: 193–203.

Wunderlich, B. 1976. **Macromolecular Physics. Vol. 2: Crystal Nucleation, Growth, Annealing.** Academic Press. New York, NY, USA. 461 pp.